

CONJUGATED HEAT TRANSFER IN THE SPATIAL LAMINAR-TURBULENT TRANSITION

William I. Machaca Abregu^{a,b}, Federico E. Teruel^{a,b,c} and Enzo A. Dari^{a,b,c}

^a*Instituto Balseiro, Universidad Nacional de Cuyo, Av. Ezequiel Bustillo 9500, 8400 San Carlos de Bariloche, Rio Negro, Argentina.*

^b*Departamento de Mecánica Computacional, Centro Atómico Bariloche, Av. Ezequiel Bustillo 9500, 8400 San Carlos de Bariloche, Rio Negro, Argentina.*

^c*CONICET, Centro Atómico Bariloche, Av. Ezequiel Bustillo 9500, 8400 San Carlos de Bariloche, Rio Negro, Argentina.*

Keywords: Laminar-turbulent transition, Conjugate Heat Transfer, Incompact3D, DNS.

Abstract. The conjugate heat transfer in the spatial laminar-turbulent transition is studied using direct numerical simulation (DNS). For that purpose, a three-dimensional (3D) module that solves the conduction equation in a solid is implemented and coupled to the Navier-Stokes equation solver Incompact3d. This module allowing to avoid an artificial imposition of the thermal boundary condition right on the fluid. First, the code is validated testing fully developed laminar flow conditions ($Re = 100$, $Pr = 0.71$). In this regime, results are very well compared with an in-house 2D code. Finally, the spatial laminar-turbulent transition at $Re = 3420$ and $Pr = 0.71$ is simulated to study the effect of the channel walls on the Nusselt number.

1 INTRODUCTION

In previous works (Machaca Abregu and Teruel, 2016, 2017), the heat transfer in the spatial laminar-turbulent transition in a rectangular channel was studied without considering the effect of the walls, that is, imposing the thermal boundary condition right on the fluid. However, it is widely recognized that this boundary condition can not mimic the heat transfer in a real situation as both, the temperature and the heat flux at the solid-fluid interface, are fluctuating quantities in a turbulent flow. For that reason, the thermal interaction between the fluid and the solid, known in the literature as conjugate heat transfer (CHT), has been described by several Authors. Tiselj et al. (2001) were the first to investigate the CHT using direct numerical simulation. They compared their results with the results of Kasagi et al. (1989), who performed similar calculation with deterministic near-wall turbulence model and numerical approach. Tiselj et al. (2001) found that previous studies underestimated the values of the wall temperature fluctuations, and concluded that with DNS calculations with CHT it can be decided which behavior should be expected in a real fluid-solid system. More recently, Flageul et al. (2015a) studied a turbulent channel flow with three thermal boundary condition: uniforme wall temperature (UWT), uniform heat flux (UHF) and conjugate heat transfer (CHT). They showed that values of the temperature fluctuations in the fluid with CHT are contained between those obtained with UHF and UWT.

As we are interested in the spatial laminar-turbulent transition phenomenon the purpose of this study is to analyze the effect of the CHT in the transitional regime, that, for the knowledge of the authors, is not know.

In the present work, a module that solves the energy equation in the walls of a rectangular channel is implemented and coupled to the Incompact3d Navier-Stokes equation solver. With this new module, the conjugate heat transfer (CHT) in the spatial laminar-turbulent transition in rectangular channels is studied numerically using direct numerical simulation (DNS). In section 2 the most important numerical aspects to carry out the simulations are presented. In section 3, the 3D module implementation is validated in laminar flow condition. Later, the results in the scenario of spatial laminar-turbulent transition for $Re = 3420$ and $Pr = 0.71$ are shown and compared with those obtained without walls. Finally, the main conclusions of the present study are presented.

2 DIRECT NUMERICAL SIMULATIONS

The numerical study of conjugate heat transfer (CHT) in the spatial laminar-turbulent transition is performed in a rectangular domain as shown in figure 1. The Navier-Stokes equations with transport of a passive scalar (temperature), and the energy equation are solved in the fluid and in the solid, respectively. For this purpose, the precise numerical tool, Incompact3d (Laizet et al., 2010; Laizet and Li, 2011), and linear stability theory (Schmid and Henningson, 2001; Schlatter, 2005; Machaca Abregu, 2015), that allows the transition from laminar flow to turbulent flow in acceptable computational times, are used.

Below are the equations that governs the hydrodynamic field and the temperature field.

2.1 Hydrodynamic equations

For the resolution of the Navier-Stokes equations, the distance, the instantaneous velocity, the pressure and the time are dimensionless with the half height of the channel h (fluid domain), the maximum velocity in the streamwise direction U_o , the density ρ and the cinematic viscosity

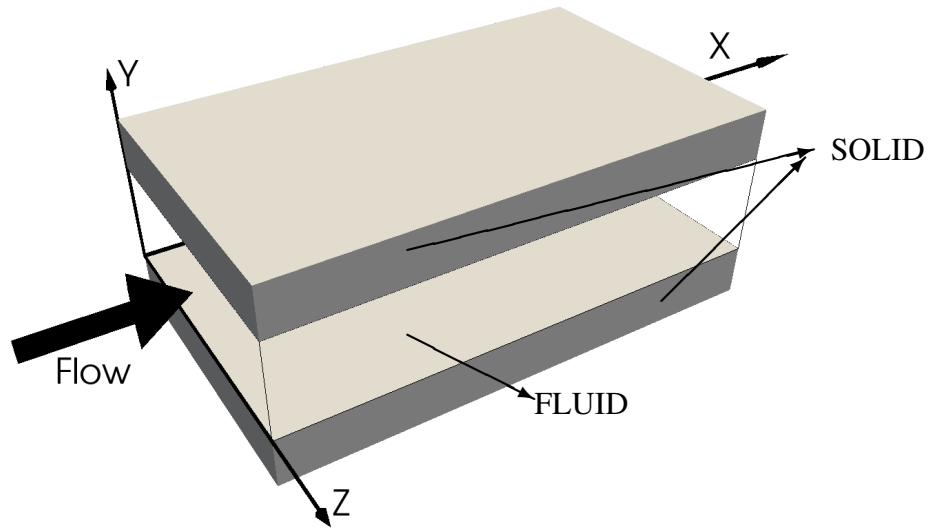


Figure 1: Sketch of the domain for the study of CHT in spatial laminar-turbulent transition.

ν . The dimensionless equation is shown below:

$$\frac{\partial \vec{u}^*}{\partial t^*} + \frac{1}{2}(\nabla(\vec{u}^* \otimes \vec{u}^*) + \vec{u}^* \cdot \nabla)\vec{u}^* = -\nabla p^* + \frac{1}{Re_o} \nabla^2 \vec{u}^*, \quad (1)$$

$$\nabla \cdot \vec{u}^* = 0, \quad (2)$$

where: $\vec{u}^* = \frac{\vec{u}}{U_o}$ is the velocity field ($\vec{u}^* = (u^*, v^*, w^*)$), $\vec{x}^* = \frac{\vec{x}}{h}$ ($\vec{x}^* = (x^*, y^*, z^*)$), $t^* = \frac{tU_o}{h}$ is the time, $p^* = \frac{p}{\rho U_o^2}$ is the pressure field, $Re = Re_o = \frac{U_o h}{\nu}$ is the Reynolds number. Note that in the equation 1 the convective term is written in its antisymmetric form. This specific form allows a better conservation of the kinetic energy for the spatial discretization used in the code (Kravchenko and Moin, 1997).

The boundary conditions are: inflow/outflow in the streamwise direction (x), periodic in z and no-slip in y . The inflow condition, in the present work, is a Poiseuille flow for laminar case and disturbed Poiseuille flow for laminar-turbulent transition case. For the outflow boundary condition, the convective condition (Lamballais, 2014) is used.

2.2 Energy equation

The general dimensionless equations of the problem (CHT) in the fluid (f) and in the solid (s) are:

$$\frac{\partial \theta_f}{\partial t^*} + u_j^* \frac{\partial \theta_f}{\partial x_j^*} = \frac{1}{RePr} \frac{\partial^2 \theta_f}{\partial x_j^{*2}}, j = 1, 2, 3 \quad (3)$$

$$\frac{\partial \theta_s}{\partial t^*} = \frac{1}{G_1 RePr} \frac{\partial^2 \theta_s}{\partial x_j^{*2}}, j = 1, 2, 3 \quad (4)$$

with boundary condition for uniform heat flux (UHF):

$$\left. \frac{\partial \theta_s}{\partial y^*} \right|_{y^*=2+L_{stop}/h} = \frac{1}{G_2}; \left. \frac{\partial \theta_s}{\partial y^*} \right|_{y^*=-L_{sbot}/h} = -\frac{1}{G_2} \quad (5)$$

$$\theta_s \Big|_{x^*=0} = 0; \theta_f \Big|_{x^*=0} = 0 \quad (6)$$

and with the conditions in the fluid/solid interface:

$$\theta_s \Big|_{y^*=2} = \theta_f \Big|_{y^*=2}; \theta_s \Big|_{y^*=0} = \theta_f \Big|_{y^*=0} \quad (7)$$

$$-\frac{\partial \theta_s}{\partial y^*} \Big|_{y^*=2} = -\frac{1}{G_2} \frac{\partial \theta_f}{\partial y^*} \Big|_{y^*=2}; -\frac{\partial \theta_s}{\partial y^*} \Big|_{y^*=0} = -\frac{1}{G_2} \frac{\partial \theta_f}{\partial y^*} \Big|_{y^*=0} \quad (8)$$

where: $\theta_s = \frac{k_f}{q''h}(T_s - T_o)$, $\theta_f = \frac{k_f}{q''h}(T_f - T_o)$, $x_j^* = x_j/h$, $t^* = (t * U_o)/h$ (U_o is the maximum velocity), $Re = \frac{U_o h}{\nu_f}$ (ν_f is the viscosity of the fluid), $Pr = \frac{\nu_f}{\alpha_f}$, $\alpha_f = \frac{k_f}{\rho_f C p_f}$, $\alpha_s = \frac{k_s}{\rho_s C p_s}$, $G_1 = \frac{\alpha_f}{\alpha_s}$ and $G_2 = \frac{k_s}{k_f}$. ρ_f is the density of the fluid, $C p_f$ is the heat capacity of the fluid, T_f is the temperature of the fluid, k_f is the conductivity of the fluid, ρ_s is the density of the solid, $C p_s$ is the heat capacity of the solid, T_s is the temperature of the solid, k_s is the conductivity of the solid, q'' is the heat flow, $L_f = 2h$ is the height of the fluid (h is the half height), L_{stop} is the height of the upper solid, L_{sbot} is the height of the lower solid, and T_o is the inlet temperature in the solid and in the fluid.

For the outflow boundary condition, the convective condition (Lamballais, 2014) and the Neumann condition is used in the fluid and in the solid, respectively.

With the equations of hydrodynamic field and thermal field, we implement the 3D module.

2.3 Numerical Implementation

The 3D module to solve the energy equation in the solid was implemented following the development carried out by Flageul et al. (2015b). For the spatial differentiation, high (sixth) order compact finite difference schemes for first and second derivatives are used. The difference schemes are adapted to implement the inflow/outflow condition in the streamwise direction. For the temporal discretization, a second order Adams-Bashford scheme is used. The imposition of the continuity of the temperature and heat flux at the solid-fluid interface at each time step is difficult to achieve without penalizing the stability of the explicit time-advance schemes. Flageul et al. (2015b) and Giles (1997) recommends imposing the boundary conditions in the following manner in the fluid domain:

$$\theta_f^{n+1} \Big|_{y^*=0} = \frac{\theta_f^n \Big|_{y^*=0} + \theta_s^n \Big|_{y^*=0}}{2}; \theta_f^{n+1} \Big|_{y^*=2} = \frac{\theta_f^n \Big|_{y^*=2} + \theta_s^n \Big|_{y^*=2}}{2} \quad (9)$$

where n is the time-step.

When the temperature of the fluid face is solved, the heat flux at the interface can be compute and imposed as boundary condition at the solid face, ensuring the continuity of this quantity. These approach is stable and first-order accurate in time (Flageul, 2015). Therefore, at the interface, in the fluid domain a Dirichlet boundary condition is imposed and, in the solid domain, a Neumann boundary condition is used (8 y 5).

3 RESULTS

The developed module is validated in the laminar regime with an in-house 2D code. After this validation, a laminar-turbulent transition with conjugate heat transfer is simulated.

3.1 Laminar validation

The conjugate heat transfer is calculated for $Re = 100$ and $Pr = 0.71$ with the 2D code that only solves the energy equation (a fully developed flow is imposed for the fluid phase) and the 3D code (Incompact3d + 3D module). This case is simulated with two different wall thicknesses to show the difference with the case without wall. The parameters of the simulations are shown in table 1.

| Case | Code | G_1 | G_2 | fluid | | solid | |
|------|------|-------|-------|-----------------------------|-----------------------------|-----------------------------|-----------------------------|
| | | | | $L_x \times L_y \times L_z$ | $n_x \times n_y \times n_z$ | $L_x \times L_y \times L_z$ | $n_x \times n_y \times n_z$ |
| I | 2D | | | 20×2 | 65×33 | | |
| II | 3D | 1 | 1 | $20 \times 2 \times 3$ | $101 \times 33 \times 8$ | $20 \times 1 \times 3$ | $101 \times 33 \times 8$ |
| III | 3D | 1 | 1 | $20 \times 2 \times 3$ | $101 \times 33 \times 8$ | $20 \times 0.5 \times 3$ | $101 \times 17 \times 8$ |
| IV | 2D | 1 | 1 | 20×2 | 65×33 | 20×1 | 65×33 |
| V | 2D | 1 | 1 | 20×2 | 65×33 | 20×0.5 | 65×17 |

Table 1: Parameters of simulations for CHT in laminar regime.

The Nussel number (see Machaca Abregu and Teruel (2016, 2017)) is shown in figure 2. It is shown that the results of the 3D code are indistinguishable that those obtained with the 2D code. This shows that our results was validated. In the same figure we show the results of UHF without solid domain (case I). It is shown also that the Nusselt number downstream of the inlet approximates to the result of UHF without solid wall when the wall thickness is reduced.

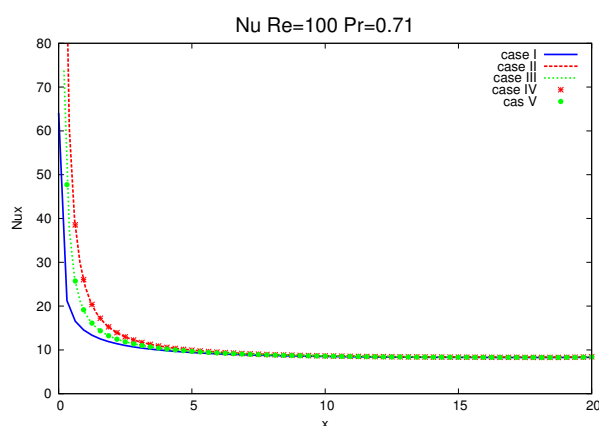


Figure 2: Comparison between 3D solutions and 2D solutions for CHT in laminar channel flow.

Considering a correct implementation of the new module to calculate CHT in Incompact3d in laminar channel flow, we continue with the calculation of the CHT in the laminar-turbulent transition. The analysis of these case is studied in the next section.

3.2 Laminar-turbulent transition

The scenario simulated correspond to a transition regime for $Re = 3420$ and $Pr = 0.71$. First the disturbances to destabilize the flow are calculated. The parameters of the disturbance are shown in the table 2,

| Re | A_{2d} | A_{3d} | w_{r2d} | w_{r3d} | β |
|------|----------|----------|-----------|-----------|---------|
| 3420 | 8% | 1% | 0.3 | 0.3 | 2.0944 |

Table 2: Perturbation parameters to calculate the disturbances to be imposed at the inlet of the channel.

with these parameters, the perturbations at the inlet of the channel flow are calculated (for a further analysis see Schmid and Henningson (2001); Schlatter (2005)). Simulations are carried out with and without solid walls (see table 3).

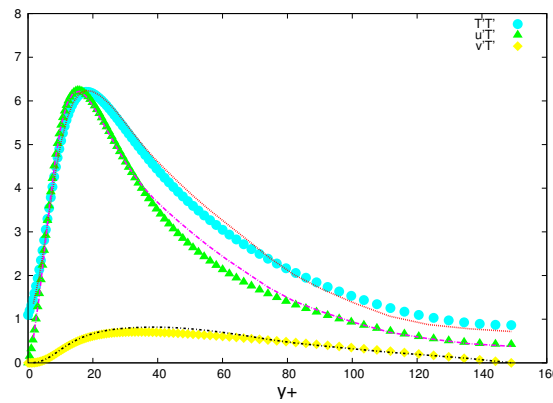
| Case | G_1 | G_2 | fluid | | solid | |
|------|-------|-------|-----------------------------|-----------------------------|-----------------------------|-----------------------------|
| | | | $L_x \times L_y \times L_z$ | $n_x \times n_y \times n_z$ | $L_x \times L_y \times L_z$ | $n_x \times n_y \times n_z$ |
| I | 1 | 1 | $120 \times 2 \times 3$ | $2401 \times 65 \times 64$ | $120 \times 1 \times 3$ | $2401 \times 33 \times 64$ |
| II | | | $120 \times 2 \times 3$ | $2401 \times 65 \times 64$ | | |

Table 3: Parameters of simulations for spatial laminar-turbulent transition with CHT (case I) and without CHT (Case II).

When the flow is in a statistically stationary state, statistics can be computed to calculate temperature fluctuation and the Nusselt number. First, we calculate the temperature fluctuation for case I in the turbulent fully developed region to be compare with a periodic simulation carried out by an independent source. Then we compare the results with CHT with the results without CHT.

3.2.1 Validation

Temperature fluctuations are shown for the case with CHT in $L_x = 117$ (turbulent zone) in figure 3. A good agreement is observed with the values calculated by Flageul (2015) in a periodic turbulent channel flow for the same flow and fluid parameters than those simulated here. This comparison suggest that our result is well resolved regarding grid requirements.



(a)

Figure 3: Temperature fluctuations in $L_x = 117$ for case I. Symbols are calculated by Flageul (2015) and lines are calculated in the present work. y^+ is the y direction in wall units.

After validating our result in turbulent zone, a comparison between two simulations (with and without CHT) are carried out.

3.2.2 Thermal analysis

The comparison between results with and without solid walls are presented for the thermal field in the transitional scenario. Figure 4a shows the Nusselt number as function of x for the cases shown in table 3 (with and without CHT). Both cases are qualitatively similar in all the regimes suggesting a weak influence of the wall on the heat transfer coefficient.

Figure 4b shows the heat flux at the interface of the channel flow ($y^* = 0$ or $y^* = 2$) for the CHT case. Naturally, there is a large difference respect to a constant heat flux imposition at the inlet. Then CHT case resembles the case of a constant wall temperature imposition. Later, in the transition region ($x = 60$) there is the larger difference respect to the case without wall. Here there is a 5% – 10% difference between the boundary condition that see the flow and the case without wall. At the outlet the convective boundary condition (Lamballais, 2014) introduce fluctuation in solid and fluid domain.

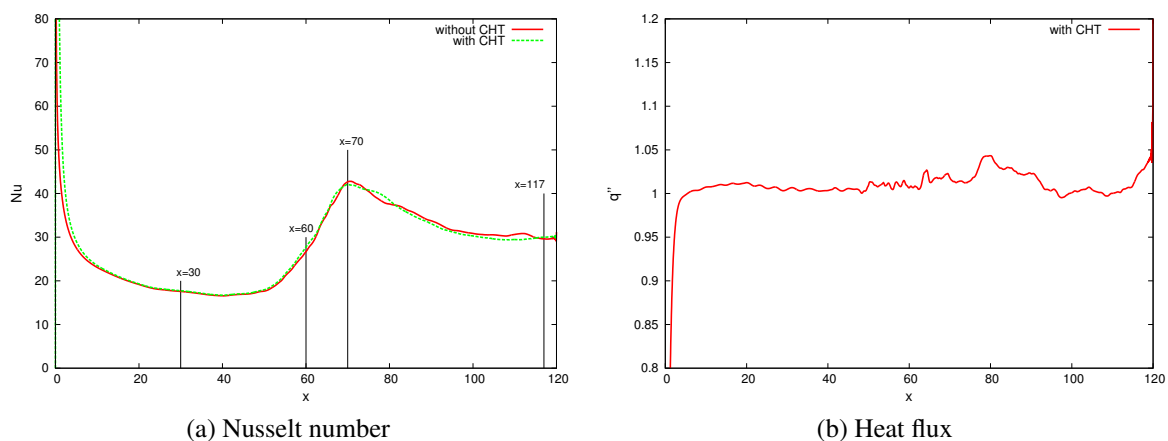


Figure 4: Nusselt number in function of x and heat flux at the walls ($y^* = 0$ or $y^* = 2$) in function of x .

The analysis of temperature statistics shows relatively larger differences between both cases than those shown in the Nusselt number. In figure 5 the temperature fluctuations are shown for four different x position. In all of them, the mayor difference is for $T'T'$ fluctuation and near the wall, where the case II is greater than case I. This fact has been found in the investigation made by Flageul (2015) for turbulent channel flows. On the other hand, in figure 5b the amplitude of the fluctuations is higher than in the other three positions. This is, probably, because in $x = 60$ exist a coherent structure (hairpin vortex (Zhou et al., 1999, 1996)). This structure increase the kinetic energy through the sweep and ejection events (Guo et al., 2010; Chen and Liu, 2011; Lu and Liu, 2012). In contrast, in $x = 70$ the values of fluctuation are less than in $x = 60$.

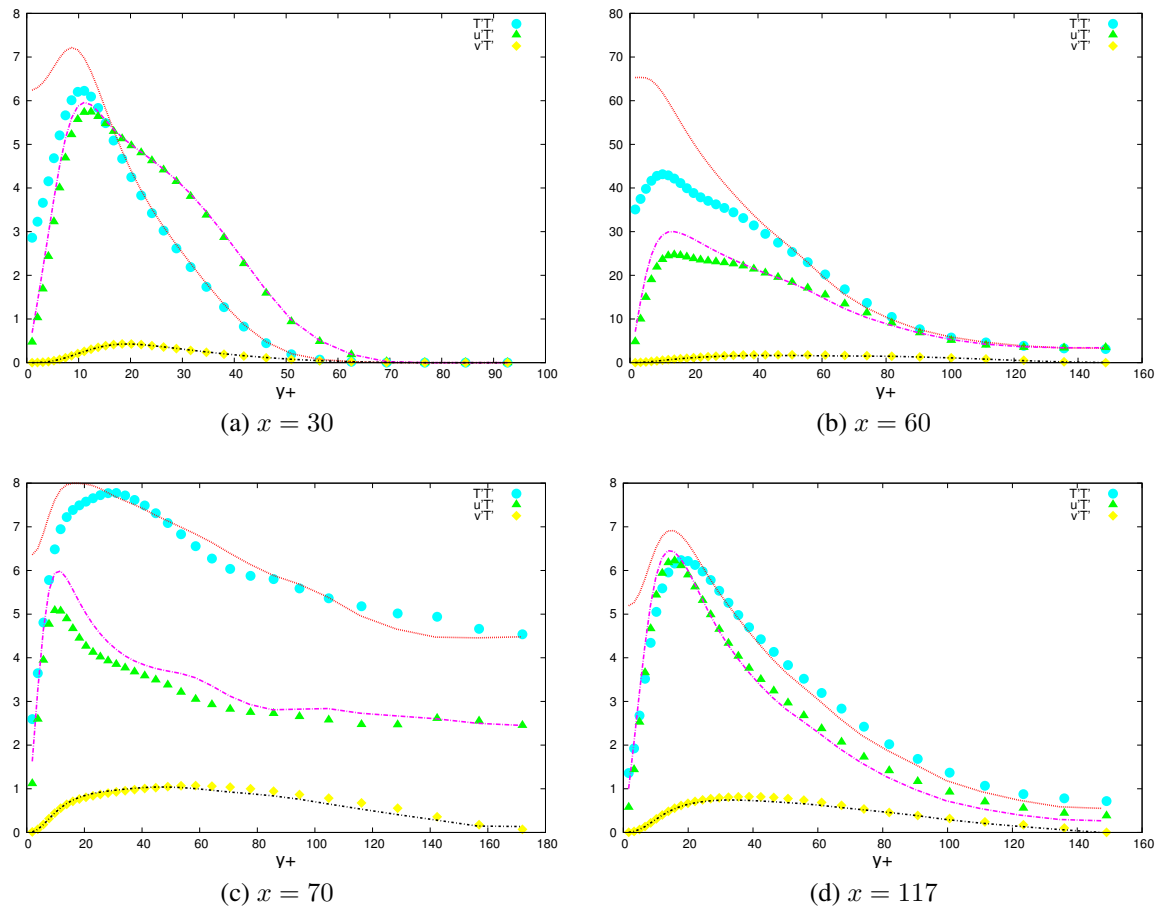


Figure 5: Temperature fluctuation for different x position. The symbols are for case I (with CHT) and the lines for case II (without CHT).

4 CONCLUSIONS

In this work, the conjugate heat transfer in spatial laminar-turbulent transition was simulated. The calculations were performed on a rectangular channel using direct numerical simulation (DNS). For this purpose, a 3D module was implemented to solve the conduction equation in the solid channel walls and it was coupled to the Incompact3d code. This code (Incompact3d + module) was validated with an in-house 2D code in laminar regime. Once the 3D code was validated, simulations were carried out, in laminar-turbulent transition, for $Re = 3420$ and $Pr = 0.71$ with and without CHT. In order to validate the results, temperature fluctuations in $x = 117$ (fully turbulent zone) for case I were calculated. These results were well compared with existing reference data. Then, the Nusselt number, the heat flux and temperature fluctuations were calculated for two cases (with and without CHT). The Nusselt number was found to be comparable between two cases from the laminar to the turbulent zone. The heat flux at the solid-fluid interface was computed to show differences of no more than 5% respect to the case without wall after the transition has started. Temperature fluctuations were also calculated to show that $T'T'$ fluctuations near the wall is higher for case I than that calculated without walls. Finally, it was shown that in $x = 60$ the temperature fluctuations are higher than the other positions, because, probably, coherent structures (hairpin vortex) governs this zone. This results can be employed to improve the design of thermal devices and, also, improve the existing RANS

and LES models.

For the case analyzed, the data obtained suggest that the CHT case does not introduce relevant difference in the heat transfer coefficient in the transition and turbulent regime respect to the case without walls.

REFERENCES

- Chen L. and Liu C. Numerical study on mechanisms of second sweep and positive spikes in transitional flow on a flat plate. *Computers and Fluids*, 40:28–41, 2011.
- Flageul C. *Création de bases de données fines par simulation directe pour les effets de la turbulence sur les transferts thermiques pariétaux*. PhD Tesis, Université de Poitiers, France, 2015.
- Flageul C., Benhamadouche S., Lamballais E., and Laurence D. Dns of turbulent channel flow: can we imitate conjugate heat-transfer with a robin boundary condition? In *8th International Symposium on Turbulence, Heat and Mass Transfer*. Bosnia, 2015a.
- Flageul C., Benhamadouche S., Lamballais E., and Laurence D. DNS of turbulent channel flow with conjugate heat transfer: Effect of thermal boundary conditions on the second moments and budgets. *Int. J. of Heat and Fluid Flow*, 55:34–44, 2015b.
- Giles M. Stability analysis of numerical interface conditions in fluid-structure thermal analysis. *Int. J. Numer. Meth. Fluids*, 25:421–436, 1997.
- Guo H., Borodulin V.I., Kachanov Y.S., Pan C., Wang J.J., Lian Q.X., and Wand S.F. Nature of sweep and ejection events in transitional and turbulent boundary layers. *Journal of Turbulence*, 11(34):1–51, 2010.
- Kasagi N., Kuroda A., and Hirata M. Numerical investigation of near-wall turbulent heat transfer taking into account the unsteady heat conduction in the solid wall. *J. Heat Transfer*, 111:385–392, 1989.
- Kravchenko A.G. and Moin P. On the effect of numerical errors in Large Eddy simulation of turbulent flows. *J. Comp. Phys.*, 131:310–332, 1997.
- Laizet S., Lamballais E., and Vassilicos J.C. A numerical strategy to combine high-order schemes, complex geometry and parallel computing for high resolution DNS of fractal generated turbulence. *Computers and Fluids*, 39-3:471–484, 2010.
- Laizet S. and Li N. Incompat3d, a powerful tool to tackle turbulence problems with up to $O(10^5)$ computational cores. *Int. J. of Numerical Methods in Fluids*, 67-11:1735–1757, 2011.
- Lamballais E. Direct numerical simulation of a turbulent flow in a rotating channel with a sudden expansion. *J. Fluid Mech.*, 745:92–131, 2014.
- Lu P. and Liu C. DNS study on mechanism of small length scale generation in late boundary layer transition. *Physica D*, 241:11–24, 2012.
- Machaca Abregu W.I. *Esquemas compactos de alto orden para el estudio de la transferencia de calor en régimen de transición*. Tesis de Maestría en Ingeniería, Instituto Balseiro, Universidad Nacional de Cuyo, Argentina, 2015.
- Machaca Abregu W.I. and Teruel F.E. *Transferencia de calor en el régimen de transición laminar-turbulento en canales rectangulares para reynolds moderados*. ENIEF 2016, Córdoba, Argentina, 2016.
- Machaca Abregu W.I. and Teruel F.E. *Estudio de la transferencia de calor en el régimen de transición temporal laminar-turbulento en canales angostos para Reynolds moderados*. ENIEF 2017, La Plata, Argentina, 2017.
- Schlatter P.C. *Large-Eddy simulation of transition and turbulence in wall-bounded shear flow*. PhD Tesis, Swiss Federal Institute of Technology, Zurich, 2005.

- Schmid P.J. and Henningson D.S. Stability and Transition in Shear Flows. In *Applied Mathematical Sciences*, volume 142. Springer, 2001.
- Tiselj I., Bergant R., Mavko B., Bajsic I., and Hetsroni I. Direct numerical simulation of turbulent heat transfer in channel flow with heat conduction in the solid wall. *J. Heat Transfer*, 123(5):849–857, 2001.
- Zhou J., Adrian R.J., and Balachantar S. Autogeneration of near-wall vortical structures in channel flow. *Physics of Fluids.*, 8(1):288–290, 1996.
- Zhou J., Adrian R.J., Balachantar S., and Kendall T.M. Mechanisms for generating coherent packets of hairpin vortices in channel flow. *J. Fluid Mech.*, 387:353–396, 1999.